Connected Physical Models controlled with the Sensel Morph

Silvin Willemsen, Nikolaj Andersson, Stefania Serafin
Multisensory Experience Lab,
Aalborg University Copenhagen
Copenhagen, Denmark
{sil, nsa, sts}@create.aau.dk

Stefan Bilbao
Acoustics and Fluid Dynamics Group/Music,
University of Edinburgh
Edinburgh, UK
sbilbao@staffmail.ed.ac.uk

ABSTRACT

Lorum Ipsum

1. INTRODUCTION

The behaviour of musical instruments can be well defined by partial differential equations (PDEs) [1].

Finite-difference schemes (FDSs)

The physical models (PMs) used as a case study in this project are the stiff string and the plate.

On top of all this, we have used the expressive control surface Sensel Morph [2]

This paper is structured as follows: Section 2 describes the PMs used in the implementation and Section 3 shows the FDSs used to digitally implement these models. Furthermore, Section 4 will describe an energy analysis of a connected string-plate system, Section 5 will show how to implement the FDSs, Section 6 shows several different configurations of PMs inspired by real musical instruments and finally Section 7 and Section 8 will discuss and conclude upon the work shown in this paper.

2. MODELS

In this section, the partial differential equations for the damped stiff string and the plate will be presented.

2.1 Stiff string

The state $u = u(x,t)$ describes the transverse displacement of the string. The subscript for u denotes a single derivative with respect to time t or space x respectively. The partial differential equation for the damped stiff string is defined as [3]

$$u_{tt} = \gamma^2 u_{xx} - \kappa^2 u_{xxxx} - 2\sigma_0 u_t + 2\sigma_1 u_{txx}, \quad (1)$$

where γ is wave-speed [m/s], $\kappa = \sqrt{EI/\rho AL^4}$ is a stiffness parameter and $\sigma_0 \geq 0$ and $\sigma_1 \geq 0$ are frequency-dependent and frequency-independent damping respectively.

We can add an excitation term to extend Equation (1) to a bowed string [3]

$$u_{tt} = ... - \delta(x - x_\text{B}) F_\text{B} \phi(v_\text{rel}), \quad \text{with} \quad (2)$$
$$v_\text{rel} = u_t(x_\text{B}) - v_\text{B} \quad (3)$$

where $F_\text{B} = f_\text{B}/\rho AL$ is the excitation function [m/s^2], with bowing force f_B [N], material density ρ [kg/m^3], cross-sectional area A [m^2] and string length L [m]. The relative velocity v_rel is defined as the difference between the velocity of the string at bowing point x_B and the bowing velocity v_B [m/s] and ϕ is a friction characteristic, which has been chosen to be [3]

$$\phi(v_\text{rel}) = \sqrt{2a} v_\text{rel} e^{-a v_\text{rel}^2 + 1/2}. \quad (4)$$

Furthermore,

$$\delta(x - x_\text{B}) = \begin{cases} 1, & \text{if } x = x_\text{B} \\ 0, & \text{otherwise,} \end{cases} \quad (5)$$

which, when multiplied onto the excitation, applies it to point x_B on the string.

2.2 Plate

In the case of a plate, the state $u = u(x,y,t)$ is now defined over two spatial dimensions. The PDE for a damped plate is [3]

$$u_{tt} = -\kappa^2 \Delta\Delta u - 2\sigma_0 u_t + 2\sigma_1 \Delta u_t, \quad (6)$$

where $\kappa = \sqrt{Eh^2/12\rho(1-\nu)}/L_x L_y$ is again a stiffness parameter with Young's modulus E [N/m^2], plate-thickness h [m], material density ρ [kg/m^3], unit-less Poisson's ratio $\nu = 0.3$, and horizontal and vertical length of the plate L_x and L_y [m]. Furthermore, Δ represents the 2D Laplacian (also see Equation (16)). Just like in the case of the string, an extra term can be added as an input:

$$u_{tt} = ... + F_\text{e} E_\text{e}, \quad (7)$$

where $F_\text{e} = f_\text{e}/\rho h L_x L_y$ with excitation force f_e [N] and E_e are an excitation function and the excitation area respectively.

2.3 Connections

Adding connections between different PMs, further referred to as elements, adds another term to Equation (2) or (7)

$$u_{tt} = ... + F_\alpha E_\alpha, \quad (8)$$
$$u_{tt} = ... + F_\beta E_\beta, \quad (9)$$

where F_α and F_β are the forces of the connection at connection areas E_α and E_β respectively. If the a connection area consists of only one point, E reduces to $\delta(x - x_c)$ where x_c is the point of connection. We use the implementation as presented in [4] where the connection between two elements is a non-linear spring. The forces it imposes on the elements it connects - denoted by α and β - are defined as

$$F_\alpha = -\omega_0^2\eta - \omega_1^4\eta^3 - 2\sigma_\times\eta_t, \tag{10}$$
$$F_\beta = -M_{\alpha/\beta}F_\alpha, \tag{11}$$

where ω_0 and ω_1 are the linear and non-linear spring coefficients respectively, $\sigma_\times$ is the damping factor, $M_{\alpha/\beta}$ is the mass ratio between the two elements and η is the relative displacement between the connected elements at the point of connection. The subscript t again denotes a time derivative.

3. FINITE-DIFFERENCE SCHEMES

To be able to digitally implement the continuous equations shown in the previous section, they need to be approximated. The models can be discretised at times $t = nk$, where $n \in \mathbb{W}$ and $k = 1/f_\text{s}$ is the time-step with sample-rate f_s and locations $x = lh$, where $l \in [0, N]$ with N being the total number of points and h is the grid-spacing of the model which is calculated differently for each model (see sub-sections below). The discretised variable u_l^n is $u(x,t)$ at the nth time step and the lth point on the string. In the case of a plate, the second spatial dimension is discretised using $x = lh$ where $l \in [0, N_x]$ with N_x being the total horizontal number of points and $y = mh$ where $m \in [0, N_y]$ with N_y being the total vertical number of points. Approximations for the derivatives in the equations found in Section 2 are described in the following way:

When approximating the PDEs shown in Section 2, we use operators

$$\delta_{xx}u_l^n = \frac{1}{h^2}\big(u_{l+1}^n - 2u_l^n + u_{l-1}^n\big), \tag{12}$$
$$\delta_{t-}u_l^n = \frac{1}{k}\big(u_l^n - u_l^{n-1}\big), \tag{13}$$
$$\delta_{t\cdot}u_l^n = \frac{1}{2k}\big(u_l^{n+1} - u_l^{n-1}\big), \tag{14}$$
$$\delta_{tt}u_l^n = \frac{1}{k^2}\big(u_l^{n+1} - 2u_l^n + u_l^{n-1}\big), \tag{15}$$
$$\delta_\Delta u_{l,m}^n = \frac{1}{h^2}\big(u_{l,m+1}^n + u_{l,m-1}^n + u_{l+1,m}^n + \tag{16}$$
$$u_{l-1,m}^n - 4u_{l,m}^n\big). \tag{17}$$

3.1 Stiff String

Equation (2) can be approximated using

$$\begin{aligned}\delta_{tt}u_l^n =& \gamma^2\delta_{xx}u_l^n - \kappa^2\delta_{xx}\delta_{xx}u_l^n - 2\sigma_0\delta_{t\cdot}u_l^n \\ &+ 2\sigma_1\delta_{t-}\delta_{xx}u_l^n - \delta_{x_\text{B}}F_\text{B}\phi(v_\text{rel}),\end{aligned} \tag{18}$$

where $\delta_{x_\text{B}} = \delta(x - x_\text{B})$ (see Equation (5)) and

$$v_\text{rel} = \delta_{t\cdot}u(x_\text{B}) - v_\text{B}. \tag{19}$$

For our implementation, clamped boundary conditions were used, defined as:

$$u = u_x = 0 \quad \text{where} \quad l = \{0, N\}. \tag{20}$$

For stability reasons, the grid-spacing needs to abide the following condition

$$h \geq \sqrt{\frac{\gamma^2k^2 + 4\sigma_1k + \sqrt{(\gamma^2k^2 + 4\sigma_1k)^2 + 16\kappa^2k^2}}{2}}. \tag{21}$$

The closer h is to this limit, the higher the quality of the implementation. The number of points N can then be calculated using

$$N = h^{-1}. \tag{22}$$

3.2 Plate

Equation (7) can be approximated using

$$\begin{aligned}\delta_{tt}u_{l,m}^n =& -\kappa^2\delta_\Delta\delta_\Delta u_{l,m}^n - 2\sigma_0\delta_{t\cdot}u_{l,m}^n \\ &+ 2\sigma_1\delta_t\delta_\Delta u_{l,m}^n + F_\text{e}E_\text{e}\end{aligned} \tag{23}$$

In the case of the plate, we set the number of horizontal and vertical points and calculate grid spacing h from that using

$$h = \frac{\sqrt{N_x/N_y}}{N_x}. \tag{24}$$

3.3 Connections

$$F_\alpha = -\omega_0^2\mu_{t\cdot}\eta - \omega_1^4\eta^2\mu_{t\cdot}\eta - 2\sigma_\times\delta_{t\cdot}\eta, \tag{25}$$
$$F_\beta = -M_{\alpha/\beta}F_\alpha, \tag{26}$$

The relative displacement η between α and β can be calculated as

$$\eta^n = h_\alpha u_{\alpha,x_\alpha}^n - h_\beta u_{\beta,x_\beta}^n, \tag{27}$$

which, in other words, is the difference between the state of element α at connection point x_α and the state of element β at connection point x_β scaled by their respective grid-spacings h_α and h_β.

4. ENERGY ANALYSIS

$$\begin{matrix}\mathfrak{H}\\ \mathfrak{B}\\ \mathfrak{T}\\ \mathfrak{D}\end{matrix} \tag{28}$$

5. IMPLEMENTATION

In this section, we will present how to implement the FDSs presented in Section 3 and elaborate more on the parameters used. We used C++ along with the JUCE framework for implementing the PMs and connections in real-time. The main hardware used for testing was a MacBook Pro with a 2.2 GHz Intel Core i7 processor.

Note: In this paper we have used the simple case of a single point for bowing, excitation and connections. These

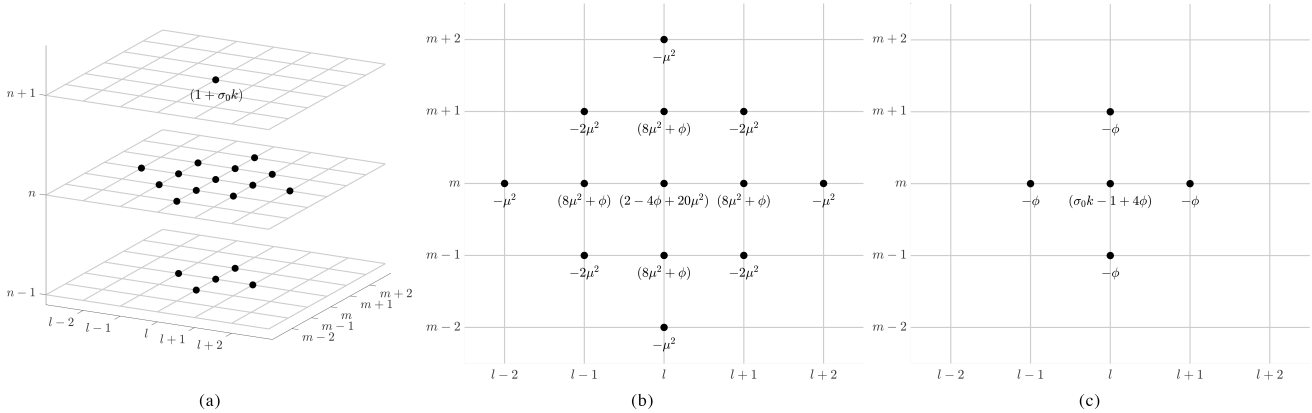

Figure 1. A visualisation of the finite-difference scheme of the plate (also see Equation (36) in Appendix A). The dots and equations represent the locations (l, m) and what these are multiplied with. (a) An overview. (b) The current time-step n. (c) The previous time-step $n - 1$.

can be extended to a bowing area, excitation area and area of connection. For more information on this, we would like to refer the reader to [4].

5.1 String

In order to implement the FDSs presented in Section 3 they need to be solved for u^{n+1}. Equation (32) found in Appendix A shows a solved finite-difference scheme of Equation (18). The wave-speed of the string is proportional to the fundamental frequency of the stiff string according to

$$\gamma = 2f_0. \tag{29}$$

This can be altered in real-time to control the pitch

The stiffness can be calculated using

$$\kappa = \frac{\sqrt{B}\gamma}{\pi}, \tag{30}$$

where $B = 0.001$ is the inharmonicity coefficient [m^{-2}].

The output is retrieved at $l = \text{floor}(0.75N)$ for all strings.

As can be seen from Equation (19) the solution for v_{rel} is implicit. It is thus necessary to use an iterative root-finding method such as Newton-Raphson [source]

$$f(v_{\text{rel}})^{i+1} = f(v_{\text{rel}})^{i} - \frac{f(v_{\text{rel}})^{i}}{f'(v_{\text{rel}})^{i}}. \tag{31}$$

This process continues until

$$f^{i+1} - f^{i} < \epsilon,$$

where $\epsilon = 10^{-4}$ is an arbitrary threshold.

5.2 Plate

A solved finite-difference scheme for Equation (23) is presented by Equation (36) in Appendix A. A visualisation of this FDS can be found in Figure 1.

6. INSTRUMENTS

In this section, several configurations of PMs and connections will be shown that are inspired by real-life instruments.

In the implementation, the string-elements are subdivided into three types: bowed, plucked and sympathetic strings. One plate is used as a body for all instruments. Each element

All instruments have

6.1 Sitar

6.2 Hurdy Gurdy

6.3 Dulcimer

User-controlled variables:

- Bowing position
- Bow force
- Bow velocity
- Connection points
- Finger position (pitch)

The vertical velocity of the finger is linked to the bow velocity with a maximum of $V_{\text{b}} = 0.2$ m/s and the finger force is linked to the excitation function with a maximum of 100 m/s^2.

6.4 Sensel Morph

Something about the sensel morph

6.4.1 Mapping strategies

Something about the different prototype mappings, and the ”final” mapping

7. DISCUSSION

8. CONCLUSION AND FUTURE WORK

Acknowledgments

We would like to thank...

9. REFERENCES

[1] S. Bilbao, B. Hamilton, R. Harrison, and A. Torin, "Finite-difference schemes in musical acoustics: A tutorial." *Springer handbook of systematic musicology*, 2018.

[2] Sensel Inc. (2018) Sensel morph. [Online]. Available: https://sensel.com/

[3] S. Bilbao, *Numerical Sound Synthesis, Finite Difference Schemes and Simulation in Musical Acoustics*. John Wiley and Sons, Ltd, 2009.

[4] ——, "A modular percussion synthesis environment," *Proc. of the 12th Int. Conf. on Digital Audio Effects (DAFx-09)*, 2009.

10. APPENDIX A

10.1 Finite-Difference Scheme String

Solving Equation (18) for u_l^{n+1} we obtain

$$\begin{aligned}(1+\sigma_0 k)u_l^{n+1} &= 2u_l^n - (1-\sigma_0 k - 2\psi)u_l^{n-1} \\ &+ (\lambda^2+\psi)(u_{l+1}^n - 2u_l^n + u_{l-1}^n) \\ &- \mu^2(u_{l+2}^n - 4u_{l+1}^n + 6u_l^n - 4u_{l-1}^n + u_{l-2}^n) \\ &+ \psi(u_{l+1}^{n-1} + u_{l-1}^{n-1}) \\ &- k^2\delta_{l_e} F_{\mathrm{B}}\phi(v_{\mathrm{rel}}),\end{aligned} \tag{32}$$

where

$$\lambda = \frac{\gamma k}{h},\quad \mu = \frac{\kappa k}{h^2},\quad \psi = \frac{2\sigma_1 k}{h^2} \quad \text{and} \quad \delta_{l_e} = \delta(x - x_{l_e}).$$

We can iteratively solve v_{rel} using (31):

$$\begin{aligned}f(v_{\mathrm{rel}}) =& F_{\mathrm{B}}\sqrt{2a}v_{\mathrm{rel}}e^{-av_{\mathrm{rel}}^2+1/2} \\ &+ \frac{2v_{\mathrm{rel}}}{k} + 2\sigma_0 v_{\mathrm{rel}} + b,\end{aligned} \tag{33}$$

and the derivative with respect to v_{rel} is

$$\begin{aligned}f'(v_{\mathrm{rel}}) =& F_{\mathrm{B}}\sqrt{2a}(1-2av_{\mathrm{rel}}^2)e^{-av_{\mathrm{rel}}^2+1/2} \\ &+ \frac{2}{k} + 2\sigma_0,\end{aligned} \tag{34}$$

where a is a free variable (in our implementation set to 100) and

$$\begin{aligned}b =& \frac{2}{k}v_{\mathrm{B}} - \frac{2}{k^2}(u_{x_{\mathrm{B}}}^n - u_{x_{\mathrm{B}}}^{n-1}) - \frac{\gamma^2}{h^2}(u_{x_{\mathrm{B}}+1}^n - 2u_{x_{\mathrm{B}}}^n + u_{x_{\mathrm{B}}-1}^n) \\ &+ \frac{k^2}{h^2}(u_{x_{\mathrm{B}}+2}^n - 4u_{x_{\mathrm{B}}+1}^n + 6u_{x_{\mathrm{B}}}^n - 4u_{x_{\mathrm{B}}-1}^n + u_{x_{\mathrm{B}}-2}^n) \\ &+ 2\sigma_0 v_{\mathrm{B}} - \frac{2\sigma_1}{kh^2}((u_{x_{\mathrm{B}}+1}^n - 2u_{x_{\mathrm{B}}}^n + u_{x_{\mathrm{B}}-1}^n) \\ &- (u_{x_{\mathrm{B}}+1}^{n-1} - 2u_{x_{\mathrm{B}}}^{n-1} + u_{x_{\mathrm{B}}-1}^{n-1})).\end{aligned} \tag{35}$$

10.2 Finite-Difference Scheme Plate

Solving Equation (23) for u_l^{n+1} we obtain

$$\begin{aligned}(1+\sigma_0 k)u_{l,m}^{n+1} &= (2-4\psi+20\mu^2)u_{l,m}^n \\ &- \mu^2(u_{l,m+2}^n + u_{l,m-2}^n + u_{l+2,m}^n + u_{l-2,m}^n) \\ &- 2\mu^2(u_{l+1,m+1}^n + u_{l+1,m-1}^n + u_{l-1,m+1}^n + u_{l-1,m-1}^n) \\ &+ (8\mu^2+\psi)(u_{l,m+1}^n + u_{l,m-1}^n + u_{l+1,m}^n + u_{l-1,m}^n) \\ &+ (\sigma_0 k - 1 + 4\psi)u_{l,m}^{n-1} \\ &- \psi(u_{l,m+1}^{n-1} + u_{l,m-1}^{n-1} + u_{l+1,m}^{n-1} + u_{l-1,m}^{n-1}) \\ &+ k^2\delta_{l_e,m_e}F_e,\end{aligned} \tag{36}$$

where

$$\mu = \frac{\kappa k}{h^2},\quad \psi = \frac{2\sigma_1 k}{h^2} \quad \text{and} \quad \delta_{l_e,m_e} = \delta(x-x_{l_e}, y-y_{m_e}).$$